Abstracts

Abstracts in this section pertain to papers presented at the Metabolic Imaging with NMR, SPECT, and PET Symposium, March 3–6, 1986, West Palm Beach, Florida. Program Chairman: Peter D. Esser, PhD.

Utilization of MR Images for Structure Identification and Analysis in PET. A. Apicella, D. Smith, J. Chang, W. Barker, R. Duara. *Mount Sinai Medical Center, Miami Beach, FL.*

Although identification of anatomic boundaries of specific brain regions in positron emission tomography (PET) images is of great importance, no single method has been generally accepted. Patients with neurologic diseases that would benefit from PET studies would invariably also require imaging of brain structure by x-ray computed tomography or magnetic resonance (MR). We describe here a method that allows superimposition of anatomic regions from an MR image onto a PET image.

Edge detection and image segmentation techniques are applied to MR images to create a set of vectors, defining boundaries between highly contrasting image regions. These vectors delineate many of the anatomic structures present in the image slice, generating a recognizable structure map. After scaling correction, this map is superimposed on the corresponding slice from PET. The operator then registers the MR overlay on the PET image, using translation and rotation operators, controlled by a joystick.

Once the overlay is positioned using such landmarks as the midline and the outer brain limits on the PET and MR images, region of interest (ROI) outlines may be projected from one imaging modality to the other. The computer retrieves data for quantitation or display in one modality corresponding to ROIs positioned on the other modality. The selection of appropriate MR images for superimposition on PET images is achieved by visual inspection (there are usually twice the number of MR as PET slices). Positioning of the head in the scanning plane is standardized by the use of the same headmold (Kearfott et al: *J Comp Assist Tomogr* 8:1217–1220, 1984) for the two scans. Results of five preliminary trials on FDG-PET images degraded to several different levels of S/N ratio show that superimposition is possible with great accuracy even for the noisiest images.

Development and Application of an Iron-52–Manganese-52m Generator System. S.C. Augustine, F.J. Steinkruger, M.A. Quaife, R.A. Quaife, R.A. Stratbucker, R.S. Markin. *University of Nebraska Medical Center, Omaha, NE; and Los Alamos National Laboratory, Los Alamos, NM.*

An iron-52-manganese-52m (^{52}Fe-^{52}Mn) generator system was developed and applied n the study of the role of divalent cations in intermediary myocardial metabolism. Iron-52 produced at the Los Alamos Meson Physics Facility using 800 MeV proton spalation of an Ni target was separated through electrochemical dissolution and recovered through reversed-phase extraction chromatography [Fe(III)] with tri-n-butyl phosphate on silica gel. The ^{52}Fe was loaded on an anion exchange resin column. The integrity and behavior of the column were tested by extraction at intervals over a 96-hr period. The standard ion exchange column was subsequently modified to allow remote loading and elution. Several adjustments in the original generator design were instituted following initial application. Shielding modifications were made to enhance radiation safety aspects of column loading and elution. Exposure rates for personnel involved in the preparation were measured and calculated. Air lock problems were mitigated by development of a wet column configuration. The integrity of the column was maintained over the 96-hr period by testing for ^{52}Fe breakthrough. Radiation exposure to personnel in the area was reduced through modification of generator design. Repetitive elution was facilitated through the foregoing modification.

Salvage of Reperfused Myocardium Detected by Sequential PET. S.R. Bergmann, K.A.A. Fox, R.M. Knabb, B.E. Sobel. *Washington University, St. Louis, MO.*

To determine whether sequential assessment of myocardial metabolism and perfusion by positron emission tomography (PET) permits detection of salvage of ischemic, jeopardized myocardium by pharmacologic interventions, streptokinase was administered 2 hr after coronary thrombosis in eight dogs, and diltiazem (15 μg/kg/min i.v. for 24 hr) initiated 30 min prior to streptokinase in nine others. Myocardial blood flow (MBF) assessed tomographically with the $H_2{}^{15}O/C^{15}O$ technique previously validated in our laboratory was not different between the two groups after coronary occlusion. Diltiazem did not alter MBF during reperfusion. Infarction in jeopardized zones assessed tomographically with carbon-11 (^{11}C) palmitate was maximal in ten control dogs with persistent occlusions (28 ± 11% (s.d.) of the left ventricle), diminished by thrombolysis alone (17 ± 10%), and minimal after thrombolysis and concomitant diltiazem (9 ± 7%, $p < 0.05$ for each comparison). In ten other dogs studied over 4 wk with PET, MBF in jeopardized zones decreased to 18 ± 4% of normal with initial ischemia, averaged 82 ± 25% 1 hr after thrombolysis, but was reduced to 37 ± 16% of control 24 hr later. Flow 1 wk after lysis in jeopardized zones was 70 ± 5% of normal and persisted at the same level for the duration of the study. With ischemia, ^{11}C activity in jeopardized myocardium varied from 14–50% of normal despite similar reduction of flow. Uptake of [^{11}C]palmitate after reperfusion presaged enhanced uptake of palmitate at 4 wk ($r = 0.87$). Thus, recovery of myocardium subjected to ischemia and pharmacologic intervention can be assessed with sequential PET, providing a strategy for evaluation of therapies designed to reduce ischemic injury.

SPECT Study of Regional Cerebral Blood Flow in Dementia. F.J. Bonte, M.D. Devous, Sr., H.H. Chehabi, E.D. Ross. *The University of Texas Health Science Center at Dallas, TX.*

To assess the role of single photon emission computed tomography (SPECT) determination of regional cerebral blood flow (rCBF) in the dementias, especially Alzheimer's disease (AD), we used a rotating, 4-detector SPECT and

inhaled xenon-133 to study 36 patients with probable AD. Of these, six had dementias of other causes, including multi-infarct dementia (MID), and six had normal studies. The remaining 24 patients (ages 50 to 93 yr) had abnormal studies. A tomographic section 6 cm above the cantho-meatal line was divided into frontal (F), parietal, temporal (T), and occipital cortical regions of interest (ROIs) and rCBF (±s.d.) was determined within each ROI as well as each hemisphere (HEM), and the entire section, in ml/min/100 g. Results were compared with rCBF derived from similar ROI in 13 normal volunteers (N), ages 50 to 71 yr. HEM and whole-section rCBF were lower in AD than in N (59 ± 10 vs. 65 ± 9, $p = 0.05$, t-test). In addition, there was reduced flow to T ROI in AD, compared with N (left (L): $p = 0.02$; right (R): $p < 0.05$). More significant was the ratio of rCBF in T ROI to HEM ROI. In N, L T/L HEM = 0.97 ± 0.03; R T/R HEM = 1.0 ± 0.04, but in AD L T/L HEM = 0.88 ± 0.04 (t-test, $p < 0.001$); R T/R HEM = 0.92 ± 0.05 ($p < 0.001$). In 5/24 pts one or both F ROI were abnormally low, but F/HEM ratios were not abnormal. AD is characterized by a generally symmetrical and significant relative reduction of flow in an ROI that represents inferior parietal and superior temporal lobe segments, with occasional frontal flow reduction as well. Flow abnormalities correlate well with clinical signs. The appearance of the slice image enables easy differentiation from other dementias, especially MID.

Spectroscopy of the Effects of Lithium Isotopes on Renal Physiology. P.T. Cahill, J.A. Markisz, R.J.R. Knowles, T. Vullo, M. Hennessey, M. Okamoto, B.A. Bottger, P. Stolle, P.E. Stokes, J.P. Whalen. *The New York Hospital-Cornell University Medical Center, New York, NY.*

In order to quantitate differences in degrees of renal toxicity caused by 6-Li and 7-Li, we analyzed in vivo phosphorus-31 (^{31}P) nuclear magnetic resonance (NMR) spectra of rat kidneys. Male Wister rats were injected subcutaneously with either 6-Li or 7-Li chloride solutions (1 mg/kg twice daily) for a period of 2 wk. In vivo ^{31}P spectroscopy at 2.2 T was performed on the intact, surgically exposed kidney, placed on a specially designed surface coil. Phosphorus-31 spectra of control rats typically demonstrated seven peaks: three associated with beta, alpha and gamma ATP phosphate groups; a fourth displaying a small level of phosphocreatine (PCr); a phosphodiester peak; an inorganic phosphate peak; and a sugar phosphate peak. Spectra of 6-Li treated rats exhibited a markedly elevated PCr level and a decrease in the level of sugar phosphates, relative to the controls (using total areas). Rats treated with 7-Li had spectra that were similar to those of controls, except for elevated phosphodiester levels. In summary, the biochemical processes of rat kidneys treated with 7-Li are closer to those of the control rats than are those of the 6-Li treated group. Phosphorus-31 NMR spectroscopy appears to be a very sensitive method for following the effects for lithium isotopes on basic renal biochemical function.

A Method for Obtaining Two Sets of Metabolic Data from a Single PET Study Using [^{18}F]Fluorodeoxyglucose. J. Chang, R. Duara, W. Barker, A. Apicella. *Mt. Sinai Medical Center, Miami Beach, FL.*

A method has been developed to obtain two sets of glucose metabolic data representing two behavioral states using two [^{18}F]fluorodeoxyglucose (FDG) injections; 50 min apart. During each 50 min, a 30-min period of behavioral activation is followed by 20 min of positron emission tomography (PET) scanning. The first 20-min PET scan is used to obtain the metabolic data for the first behavioral state. Metabolic data for the second behavioral state is provided by the second PET scan after appropriate correction of residual activity from the first FDG injection [*J Nucl Med* 26:P102, 1985 (abstr)].

Advantages are: (a) provision of control-state data along with specific activation-state data in a single procedure; (b) avoidance of repositioning problems because subjects remain in the scanner; (c) short and fixed time interval between the two behavioral states; improving comparability; (d) reduced time demands on subjects and investigators.

Two subjects who performed identical behavioral tasks in each activation period showed <5% differences in global CMRglc and in the ratios rCMRglc/global CMRglc. Two subjects who performed disparate behavioral tasks in each activation period showed up to 17% alteration in global CMRglc and up to 15% alteration in the ratios rCMRglc/global CMRglc in appropriate brain lobes. The results of these preliminary studies show: (a) reproducibility of metabolic data from identical behavioral states, and (b) metabolic change in the appropriate brain lobes following specific activation tasks. This method is useful in behavioral studies and may be of value in pharmacologic activation studies using PET and FDG.

A Four-Quadrant, Multiple Focused Ring Collimator for High Performance Single Photon Tomography. W. Chang, B.M.W. Tsui, C. Tian, S. Li, J.J. Williams, K. Rezai, J.C. Ehrhardt, P.T. Kirchner. *University of Iowa Hospitals and Clinics, Iowa City, IA; and University of North Carolina, Chapel Hill, NC.*

A special collimator was designed for a multi-detector ring tomograph to achieve high performance brain single photon emission computed tomography. This collimator enables the ring tomograph to operate in a fashion similar to that of stationary detector computed tomography, creating detector fan data sampled sequentially over time. The ring collimator consists of four basically identical quadrants. Each quadrant consists of an array of individually focused collimator modules arranged in parallel. Each collimator module has a large number of small channels symmetrically focused to a point half way into the reconstruction circle. Ray interlacing among the four quadrants and the quarter ray offset technique are implemented to achieve fine linear sampling at the center of a 21-cm reconstruction circle. Because of the focusing effect of each collimator module, both high resolution and high sensitivity can be achieved at the center of the target volume. We designed a single slice tomographic system based on this collimator to achieve nominal 10-mm slice thickness, 7.5-mm full width at half maximum resolution at the center, and an expected 3,500 cps/μc/cc sensitivity for a 20-cm water phantom containing technetium-99m (^{99m}Tc). This sensitivity should be adequate for clinical imaging of most iodine-123 tracers. For ^{99m}Tc-labeled tracers, a similar collimator of higher resolution can be substituted easily into the same detector ring.

DSPECT Determination of Regional Cerebral Blood Flow at Rest and Following Diamox-Induced Vasodilatation in Pa-

tients with Arteriovenous Malformations. M.D. Devous, Sr., H.H. Batjer, S.R. White, D.R. Samson, B. Mickey, F.J. Bonte. *Nuclear Medicine Center and Division of Neurological Surgery, The University of Texas Health Science Center at Dallas, TX.*

Regional cerebral blood flow (rCBF) was determined by DSPECT of xenon-133 cerebral transit in 34 patients with documented intracranial AVM. Thirty-one (90%) were found to have ipsilateral underperfused areas suggestive of "cerebral steal." Twenty-four had contralateral low-flow areas. Six/11 patients studied pre- and postoperatively showed improvement in flow to "steal" areas. DSPECT measurement of rCBF was used to evaluate vascular reactivity in steal areas by studying patients at rest and following i.v. injection of Diamox (DMX), a carbonic anhydrase inhibitor which increases rCBF. Eight control subjects had a mean resting whole-brain flow of 72 ml/min/100 g which increased to 96 (33%) following DMX (500 mg, i.v.). All brain regions increased equivalently in these normals. AVM patients have demonstrated two patterns in response to DMX. In 7/10 patients both normal and steal areas of the brain increased rCBF in a manner similar to controls. Therefore, steal pattern was the same before and after DMX. Three/ten patients demonstrated "failed vasoreactivity" by showing further steal or inappropriately small increases in rCBF following DMX. These data indicate that DSPECT measurements of rCBF can be used to demonstrate areas of relative hypoperfusion asociated with AVM's and that pharmacologic activation can be employed to measure the vasoreactivity of hypoperfused regions.

SPECT Determination of Regional Cerebral Blood Flow in Schizophrenic Patients at Rest and During a Mental Task. M.D. Devous, Sr., J.D. Raese, J.H. Herman, R.G. Paulman, R.R. Gregory, A.J. Rush, H.H. Chehabi, F.J. Bonte. *Nuclear Medicine Center and Department of Psychiatry, The University of Texas Health Science Center at Dallas, TX.*

Regional cerebral blood flow (rCBF) was measured by single photon emission computed tomography (SPECT) of xenon-133 washout in 30 schizophrenic patients (SCHZ), 19 mixed psychiatric patients (MIX) and 30 normal volunteers. Frontal hypoperfusion (HYP) was observed in 43% of all SCHZ and in only 11% of MIX ($X^2 = 4.22$, $p < 0.05$). Temporal lobe HYP was the second most common rCBF abnormality. For SCHZ with abnormal rCBF images (18/30), frontal HYP was present in 80% of paranoid patients but only 29% of nonparanoid patients. Temporal lobe HYP was present in 7% of paranoid patients and 27% of nonparanoid patients. Significant correlations with neuropsychological function were demonstrated between performance on the Wisconsin Card Sort (WCS) and left frontal rCBF ($r = 0.66$), and poor correlation between frontal rCBF and Luria-Nebraska rhythm scale (sensitive to temporal lobe function) ($r = -0.02$). In contrast, left and right temporal rCBF was moderately correlated with rhythm scale performance ($r = -0.52$ left, $r = -0.58$ right). rCBF was measured in 11 SCHZ at rest and while performing a short version of the WCS. Frontal rCBF was significantly lower during WCS in seven of 7 paranoid SCHZ but was not different between resting and WCS studies in four nonparanoid SCHZ. In summary, hypofrontality occurs more frequently in the resting state of paranoid than in nonparanoid SCHZ. WCS caused frontal rCBF reductions in paranoid SCHZ but not in nonparanoid SCHZ.

Metabolic Imaging of Brain Tumors with (^{18}F)-2-Deoxyglucose: Studies in 300 Cases Including a Comparison with NMR Imaging. G. Di Chiro. *National Institutes of Health, Bethesda, MD.*

Positron emission tomography (PET) using (^{18}F)-2-deoxyglucose (FDG) as a tracer has been employed in over 300 cases of brain tumor to assess their rate of glucose utilization. We have found this method to be a remarkably effective, noninvasive method for grading primary cerebral neoplasms. Not only is there a clear separation of high-grade from low-grade tumors, but there is even a statistically significant difference in FDG uptake between grades III and IV. Indeed, in an analysis of survival rate of patients with high grade tumors, we found that the PET results correlated better with length of survival than did the histologic subclassification.

On the other hand, magnetic resonance imaging (MRI) studies also performed in many of these cases, did not allow us to obtain the same type of information. MR imaging features as well as the T_1 and T_2 relaxation values were found to overlap, thus preventing discrimination among the various tumor types and grades. Even the usage of systemically administered paramagnetic agents (Gd-diethylenetriaminepentaacetic acid) failed to offer the same precise information attained by the PET-FDG method.

The critical differentiation between radiation necrosis and tumor recurrence in x-ray treated patients can only be accomplished by the PET-FDG method. Neither computed tomography nor MRI have been found useful in this regard.

Heretofore, we have relied on fine histological nuances, which are by their very nature static, for recognizing the degree of malignancy of brain tumors. The successful application of the PET-FDG method to this purpose introduces a new concept, based on highly dynamic metabolic status of the tumor as the fundamental indicator of its biologic nature.

Regiospecific Synthesis of 6-(^{18}F)-Fluoro-L-Dopa. M. Diksic, T. Chaly. *Brain Imaging Centre, Montreal Neurological Institute and Hospital, McGill University, Montreal, Quebec, Canada.*

Fluorine-18-(^{18}F) labeled 6-fluoro-L-dopa (*1*) has been used in positron emission tomography for mapping the distribution of dopamine in normal and pathological conditions in human brain. Several syntheses of [^{18}F]6-fluoro-L-dopa have been developed, but most of them yield two or three isomers requiring elaborate and time-consuming purification (*J Nucl Med* 25:1228, 1985 and references therein).

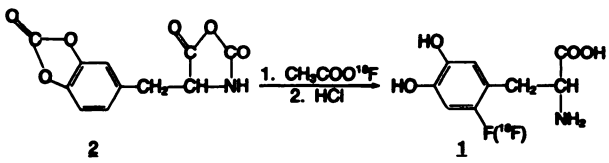

2 1

Here we describe a simple, regiospecific synthesis for introducing ^{18}F into the L-dopa molecule. The starting material (*2*) was easily prepared by reacting a suspension of L-dopa in dioxane with phosgene at room temperature. After evaporation, the residue containing compound (*2*) was dissolved in dry acetonitrile and reacted with [^{18}F]CH_3COOF (gas). At the end of bubbling the solvent was evaporated, protecting groups removed with 2N HCl, and the liquid evaporated under

reduced pressure. The residue was dissolved in water and passed through a silica column to remove, if any, F^- and through a high performance liquid chromatography (HPLC) column (RP-18) using H_2O + 0.5% AcOH + 0.01% NH_4OAc to remove a side product of the reaction. The synthesis required about 50 min and had a radiochemical yield of about 15% (EOS). Fluorine-19 nuclear magnetic resonance (NMR) showed the presence of more than 98% of 6-fluoro-dopa and, if any, less than 2% of 2-and 5-fluoro-L-dopa combined in the final radiopharmaceutical. Fluorine-19 NMR and HPLC elution volume were compared with an authentic sample of 6-fluoro-L-dopa provided by Dr. K. Kirk (NIH). Supported by the MRC.

Fluorodeoxyglucose Rate Constants and Oxidative Metabolism in Primary Gliomas Measured with PET. M. Diksic, J. Tyler, A.C. Evans, M. Kirikae, E. Meyer, Y.L. Yamamoto, J.-G. Villemure, W. Feindel. *Brain Imaging Center, Montreal Neurological Institute and Hospital, McGill University, Montreal, Quebec, Canada.*

The relationship between supply (blood flow) and utilization of nutrients to brain tumors must be determined in order to evaluate tumor metabolic state. The possibility of monitoring in vivo changes in this interrelationship during tumor therapy could influence the success of treatment.

We have measured rate constants (k_1^* to k_3^*), glucose and oxygen utilization, blood flow, and blood volume in eight patients with malignant gliomas before treatment. Areas of very low activity indicating tissue necrosis were not used for regions of interest. Rate constants and blood volume were fitted in a four variable model to tissue curves during the first 40 min after a prolonged bolus (~2 min) injection of (^{18}F)-2-fluorodeoxyglucose. Rate constants were generally higher in the tumor than in contralateral brain. However, the ratio of k_3^*/k_2^* (related to the lumped constant stability) is similar in the tumor and in contralateral gray matter (averages were 0.30 in tumor and 0.33 in gray matter). Two patients had ratios significantly higher (0.48, $p < 0.01$) and lower (0.21, $p. < 0.05$) than the mean level. Regional blood flow, blood volume, oxygen extraction, and oxygen utilization were measured by an equilibrium method using oxygen-15-labeled gases. A significant increase ($p < 0.05$) was found in glucose utilization of the tumor when regional rate constants were used instead of rate constants measured in normal volunteers. Our findings showed no significant difference in the blood volume in the viable part of the tumor as compared with contralateral gray matter. This limited number of cases revealed that the glucose and oxygen utilization, oxygen extraction fraction and blood flow are lower ($p < 0.05$) in untreated malignant gliomas as compared with contralateral gray matter.

Global Cerebral and White Matter Changes in Aging and Dementia. R. Duara, F. Yoshii, W. Barker, A. Apicella, J. Chang, J. Sheldon. *Mt. Sinai Medical Center, Miami Beach, FL.*

In 17 young normals (YN) (mean age 36.4 ± 8.8 yr), 35 elderly normals (EN) (mean age 67.0 ± 9.4 yr) and 13 patients with probable Alzheimer's disease (DAT) (mean age 71.4 ± 7.6 yr) inversion-recovery sequence magnetic resonance (MR) scans were used to measure the frontal horn index (FHI), bicaudate index (BCI) and third ventricle index (TVI) to determine the sensitivity of these indices to the processes of normal aging and dementia. To measure white matter (WM) regions, a horizontal MR slice at the level of the Foramen of Munro was used to measure the widths of the interior (AWM) and posterior (PWM) WM bundles entering the frontal and temporal-parietal lobes bilaterally.

FHI showed a nonsignificant increase of 3.4% between YN and EN, but a 15.9% increase between EN and DAT ($p < 0.02$). BCI increased by 41.3% between YN and EN ($p < 0.001$) and by 33.2% between EN and DAT ($p < 0.001$). TVI increased by 48% between YN and EN ($p = 0.003$) and by 50.6% between EN and DAT ($p = 0.001$). Unexpectedly, AWM and PWM were found to increase with age ($p < 0.02$) but no differences between DAT and EN were found. The discrepancy between FHI changes with age and the changes in BCI and TVI has been noted in other studies (Le May: *Am J Roentgenol*:143, 383–389, 1980; Meese, et al: *Neuroradiology*:19, 131–136, 1980).

Our finding of increased WM with age may explain the lack of age related changes in FHI. The frontal horns project directly into the AWM bundles; thus increases in AWM may compensate for the gray matter atrophy in the frontal regions.

The Circular Harmonic Transform Algorithm for SPECT Reconstruction. W.G. Hawkins, P.K. Leichner, N.C. Yang, T.K. Frenkel, D.M. Loudenslager. *The Johns Hopkins Hospital, Baltimore, MD.*

The purpose of this study is to demonstrate the potential for single photon emission tomographic (SPECT) reconstruction by use of the circular harmonic transform (CHT) solution of the exponential Radon transform. The CHT algorithm is based on both the 2D Fourier transform of the projection sinogram and the intrinsic solution for uniform attentuation. Accurate patient contours and correction for table attenuation are required for quantitative studies. Mathematic simulations, SPECT scans of an anthropomorphic phantom, the Jaszczak phantom and patients are used to compare the algorithm with the intrinsic algorithm based on ordinary backprojection and commercial software based on the precorrective method. The simulations and line source studies demonstrate improved resistance to streaking and a better signal-to-noise ratio for the CHT algorithm when compared with either of the other two methods. A volumetric study with the anthropomorphic phantom shows that the CHT algorithm provides better estimates of organ volume over a wide range, from pancreas (145 ml) to liver (1,950 ml). The correlation coefficient from a least squares fit of the volumes was 0.9997 (CHT) and 0.9991 (commercial software). The CHT algorithm is much less prone to nonfocal geometric distortion when compared with the commercial software. The CHT algorithm is also computationally efficient, with processing times generally less than ordinary backprojection. For SPECT protocols where the assumption of uniform attenuation is reasonable, the CHT algorithm is preferable to the algebraic-iterative methods which require long processing times.

Digital Restoration of SPECT Images of Medium-to-High Energy Photon Emitters. M.A. King, R.B. Schwinger, B.C. Penney, P.W. Doherty, J.A. Bianco. *University of Massachusetts Medical Center, Worcester, MA.*

A number of metabolic imaging agents are labeled with radionuclides which emit medium-to-high energy photons either as their primary radiation or in low abundance in

addition to their primary radiation. The imaging characteristics of these radionuclides results in single photon emission computed tomographic (SPECT) image quality which is inferior to that of technetium-99m-labeled imaging agents. Indium-111 and iodine-123 contaminated with ~4% iodine-124 were chosen to test the hypothesis that a dramatic improvement in SPECT images may be obtainable with digital image restoration of images of medium-to-high energy photon emitters. The count-dependent Metz filter is shown to be able to deconvolve the rapid drop at low spatial frequencies in the imaging system modulation transfer function (MTF) which results from the acceptance of septal penetration and scatter in the camera energy window. Use of the Metz filter was found to result in improved spatial resolution as measured by both the full width at half maximum and full width at tenth maximum for SPECT studies. Two-dimensional, prereconstruction filtering with optimized Metz filters was also determined to improve image contrast, while decreasing the noise level for SPECT studies. Dramatic improvements in image quality were observed with the clinical application of this filter to SPECT imaging.

Alteration of Contrast in NMR Images by Exogenous Agents. S.H. Koenig. *IBM T.J. Watson Research Center, Yorktown Heights, NY.*

We have been investigating the molecular basis of contrast in nuclear magnetic resonance (NMR) images and the possibility of altering this contrast by the introduction of exogeneous agents, including small chelate complexes of paramagnetic ions (e.g., Mn^{2+} and Gd^{3+}); nitroxide radicals; and (to a limited extent) fluorine-19 (^{19}F) compounds of blood substitutes. The method, called NMRD for nuclear magnetic relaxation dispersion, involves measurements of the magnetic field dependence of the longitudinal relaxation rates of the majority nuclei (typically water protons of solutions or tissue, but deuterons and ^{19}F as well) of an in vitro sample. The resulting data, an "NMRD profile," are generally obtained over a range of temperatures, this being necessary to elucidate the molecular mechanisms responsible for the observed relaxation behavior. Experience shows that the in vitro results relate directly to in vivo observations. The instrumentation, a "Relaxometer," is unique to our laboratory, and instrumentation with comparable capabilities is available in but a few other institutions. In brief, on the basis of tissue and solution results, the Mn^{2+} of Mn^{2+}-complexes introduced intravenously accumulates predominantly in the liver, separated from its chelate, and thus is potentially toxic. By contrast, strongly chelated Gd^{3+} appears in the renal medulla and, ultimately, in the urine intact. Nitroxides have the advantage that some are hydrophylic and others lipophylic; some penetrate cells and others not; some are rendered diamagnetic by metabolic processes and others made paramagnetic. Thus, nitroxides would appear to have a wide utility. Finally, ^{19}F has the advantage that its signal can be observed independently of that of protons, and that its relaxation properties can also be altered by paramagnetic agents. Results on ^{19}F and nitroxides were obtained collaboratively with, respectively, R Muller and H. Bennett.

Effect of Blood Brain Barrier Disruption on Thallium-201-DDC Distribution in Rat Brains. C. Overby, S. Vallabhajosula, R.A. Zappulla, M. Spigelman, S.J. Goldsmith. *Mount Sinai Medical Center, New York, NY.*

Thallium-201 diethyldithiocarbamate (Tl-DDC) was recently shown to be suitable for blood flow studies using single photon emission computed tomography in normal rabbits and in humans. Its usefulness in pathologic conditions, however, is not clearly determined. We have investigated the utility of Tl-DDC to measure the cerebral blood flow both in normal rats (Group 1) and in rats subjected to intracarotid etoposide infusion (Groups 2 and 3).

Blood brain barrier (BBB) disruption secondary to etoposide infusion which we have demonstrated previously was determined at the time of killing by the extent of hemispheric staining with Evans blue (EB). Tl-DDC and technetium-99m albumin microspheres (Tc-AM) were injected simultaneously into the left ventricle. The left/right hemispheric ratios of Tl-DDC were compared with that of Tc-AM.

Group	Tl-DDC	Tc-AM
1 (n = 5)	1.019 ± 0.09	1.004 ± 0.062
2 (n = 6, EB+)	0.476 ± 0.34	0.306 ± 0.270
3 (n = 2, EB−)	0.985	1.040

The decrease in the distribution of Tl-DDC and Tc-AM in the BBB disrupted hemisphere indicates that Tl-DDC adequately reflects decrease in cerebral perfusion. The distribution of Tl-DDC is similar to Tc-AM in normal animals and animals with experimentally induced abnormalities of BBB.

Optimization of Imaging Time and Filter Selection for SPECT. T.R. Simon, J.G. Triebel, J.E. Dowdey. *University of Texas Health Science Center; and VA Medical Center, Dallas, TX.*

Single photon emission computed tomography depends upon parameters whose values affect diagnostic image quality and cost as well as patient imaging and processing time. We sought optimal settings for the number of views obtained (V), counts per view (C/V), counts per sec (C/S) and temporal and spatial filters (F).

A technetium-99m-filled phantom was designed to quantitate "hot" and "cold" spot imaging. "Hot" and "cold" objects measured 19, 16, 13, 10, 6, and 3 mm. The combination of parameters studied were: 15, 30, 60, and 120V equally spaced over 360°; 100,000, 200,000, 300,000, and 400,000 C/V, 10,000, 20,000, 40,000 and 80,000 C/S at 100,000 C/V; and rectangular, Butterworth orders 3 through 7, Hamming (HM), Hann and Parzen F. Studies ranged from 3 to 48 million counts per series (MC/S). Acquisition and processing times were recorded. Images were reconstructed along three orthogonal axes displayed with the unprocessed rotating images using a gray scale with dynamic window settings. The observer twice graded each image according to the number of objects fully characterized. C/S has little effect on detection below 48 MC/S although the highest C/S generally contained the best detection scores (3 mm). Hot detection increased by 3 to 9 mm with > 15 views. Cold object detection improved less (0–3 mm) for the 3 to 6 MC/S. Increasing V variably affected detection scores by no more than 3 mm. The HM F nearly always was best. All F reconstructed 120 V in 401 sec.

Hot and cold objects were best characterized with a HM, F and > 15 V. C/V and C/S were less critical parameters for characterizing objects in the range tested.

Can NMR Contribute to the Radiopharmacokinetics of 5-Fluorouracil (5-FU) in Man? W. Wolf, J.R. Griffiths, M. Silver, H. Bruckner. *Radiopharmacy Program, University of Southern California, Los Angeles, CA; St. George's Hospital Medical School, London, UK; Siemens Medical Systems, Iselin, NJ; and Mt. Sinai Medical School, New York, NY.*

Prior work by one of us (W.W., *Nucl Med* 21: 1–7, 1982) had documented that human studies of fluorine-18-labeled 5-FU revealed differences in the biodistribution of this drug from individual to individual, specially in the early phase. It had also been documented (J.R.G., *Br J Cancer* 50: 112–117, 1984) that in vivo nuclear magnetic resonance (NMR) studies in mice allowed the detection of both 5-FU and several of its metabolites in the liver and in tumor tissue. The current studies are aimed at helping to continue evaluating the degree of responsiveness of selected tumors to 5-FU treatment, by monitoring whether individual variations in drug metabolism may allow for the recognition of responders. The key question then is: can fluorine-19 (^{19}F) NMR be performed in humans, and what might be the optimal conditions for doing so? Studies conducted in BDF-mice bearing the L-1210 Lymphocytic leukemia tumor at 1.89 T confirmed that the fluorinated products present in the liver consist mostly of the drug's catabolites. Phantom studies have been conducted at fields as low as 0.37 T, where 5-FU & selected catabolites could be readily detected at 1.5 m*M* concentrations. Optimization of appropriate surface coils and pulse sequences are currently in progress, so that further studies can help assess the relative clinical potential of ^{19}F NMR when measuring the in vivo metabolism of 5-FU in humans.

The Use of Quantitative SPECT and Physiologic Modeling for the Radiation Dosimetry of Iodine-131 Therapy for Thyroid Cancer. P.B. Zanzonico, R.E. Bigler, J.H. Hurley, D.V. Becker, C. Edwards. *New York Hospital-Cornell Medical Center, NY.*

A single photon emission computed tomography- (SPECT) based method was developed for measuring the activity (μCi) in pulmonary metastases (PM) from thyroid carcinoma following systemic therapeutic administration of iodine-131 (^{131}I). A 64 × 64 SPECT thorax study (8×10^6 cts/30 min) at 72 hr pi of 320 mCi $Na^{131}I$ was performed using a standard ECT, its standard software and "iodine" collimator, and a preprocessing sensitivity correction based on an ^{131}I flood image. The 7-mm-thick transverse images (TIs) were attenuation-corrected by Chang's method assuming an elliptical patient contour and a measured $\bar{\mu}$. The localized activity (2.5 mCi) was calculated by subtracting the mean total cts per "background" TI from the total cts in TIs having foci of activity corresponding to PM, summing the resulting net cts to yield the total PM cts, and converting cts to μCi using a calibration factor, 18.1 cts/μCi, determined from the simultaneously acquired TIs of a 0.5-mCi source. This collective quantitation method, which circumvents the difficulty of accurately de-limiting regions of interest corresponding to PM whose linear dimensions are no greater than twice the FWHM resolution of the SPECT system, is practical due to minimal background activity, attenuation, and scatter in the lung. Together with the measured time-dependent blood activity and TBR data, the PM and similarly obtained thyroid remnant data were used to optimize the exchange rates of Singh et al.'s (*J Nucl Med* 15:674, 1974) "SAAM"-implemented nonlinear iodide model. The model was used to directly calculate the $\tilde{A}$, 6.5×10^5 μCi-hr, in the PM. The $\bar{D}$, 16,800 rad, to the PM was then calculated assuming self-irradiation by nonpenetrating radiation only (which yields 0.405 g-rad/μCi-hr for ^{131}I) and using the radiographically estimated total PM mass (15 g).